Scientific paper

Ordering of Attractive Colloids near a Planar Wall: Theory and Simulation

Andrej Lajovic, Matija Tomšič and Andrej Jamnik*

University of Ljubljana, Faculty of Chemistry and Chemical Technology, Aškerčeva 5, SI-1001 Ljubljana, Slovenia

** Corresponding author: E-mail: andrej.jamnik@fkkt.uni-lj.si*

Received: 10-11-2008

Dedicated to Professor Josef Barthel on the occasion of his 80th birthday

Abstract

Structural properties of asymmetric binary sticky hard-sphere (SHS) mixture (the particular components being denoted by SHS1 and SHS2), mimicking a system of interacting spherical colloidal particles in suspensions, near a planar wall, maintaining the equilibrium with the homogeneous (bulk) phase, are investigated. The wall-SHS1 and wall-SHS2 correlations of the SHS mixture are studied using the grand canonical Monte Carlo simulation and Percus-Yevick/Ornstein-Zernike integral equation. The density profiles of particular components show interesting shapes stemming from the interplay between the steric effects and the competitive adhesion among all possible species pairs, a characteristic feature being the discontinuities in the shapes of the profiles at the distances from the wall-SHS1 and wall-SHS2 contact planes, which correspond to different sums of the multiples of particular hard core diameters. The agreement between the theoretical predictions and simulation data is fair to very good and is better for the component comprised of weakly attractive (adhesive) particles.

Keywords: Colloidal mixture, adhesive hard sphere model, inhomogeneous systems, Percus-Yevick theory, Monte Carlo simulation

1. Introduction

During recent years, considerable experimental, theoretical, and simulation work has been devoted to the investigations of the structural properties of colloids and colloid-polymer mixtures at planar interfaces.[1–11] Local ordering of the colloidal particles at the interfacial region may lead to fluid phase separation, demixing of colloidal mixtures, and may provoke important interfacial phenomena like the formation of thin layer films.[12] These phenomena are governed by the interfacial free energies between the wall (substrate) and the fluid (material) and originate from the complex interplay among the steric effects and the particular colloid-wall and colloid-colloid interactions. Their molecular interpretation therefore include various interparticle interaction potentials varying from the simplest hard sphere model, mimicking the sterically stabilized colloids, to the model that treat the colloidal particles as equally or oppositely charged hard spheres. Further, as many properties of such complex physical systems are governed by the competition between hard-core repulsion and short-range attractive interparticle interactions, various models for the so-called attractive colloids have been also frequently applied.[13–17] The simplest model, which combines both the hard-core repulsion and the short-ranged attraction, is Baxter's sticky hard sphere (SHS) fluid.[18] This model represents an extreme case of the hard sphere system with the square well in the limit of infinitely strong and infinitesimally short ranged attraction, leading to a finite interparticle attractive strength. In the sticky limit, it has an advantage over the usual square-well model and other model potentials involving a continuous attractive part in the pair potential of interaction (e.g., the hard-core attractive Yukawa (HCAY) model fluid and the Lennard-Jones (LJ) fluid) as it has been shown to possess an analytic solution to the Ornstein-Zernike (OZ) equation in the Percus-Yevick (PY) approximation[18] and in a class of other closures.[19] SHS model is therefore especially suitable for the modeling of colloidal systems as the range of inter-colloidal interactions in dispersions is

usually much shorter than the size of colloidal particles. Numerous articles appearing in the literature thus reported on the application of this model in colloid science, for example in studying the interfacial equilibrium,[20,21] phase behavior,[22] solvation phenomena,[23–25] and sedimentation equilibrium[26,27] in colloidal systems, in modeling the charged colloids,[28] and in exploring the kinetically arrested metastable gels.[29] Further, it has also been applied for a description of some complex experimental observations in colloidal systems. For example, SHS model has been used to analyze the measurements of small angle neutron and x-ray scattering of various colloidal suspensions.[30–36] In addition, numerous articles reported also integral equation studies of the properties of the one-component SHS model and related fluids near the solid surfaces and confined into the pores.[37–43] Theoretical investigations of pure adhesive fluid have been also extended to SHS mixtures of arbitrary size and adhesion strength.[44–46] An example of a two-component mixture has been applied to model gelation in a concentrated dispersion of colloidal particles,[47] solvent-mediated forces between colloidal particles in a mixed solvent,[48] and the intermicellar attractive interaction in a solution containing reverse micelles.[49]

Purely theoretical treatments of SHS model have been accompanied by computer simulations. Because of the impulse character of the adhesive potential special modifications of the conventional simulation technique rendering possible the sampling of the contact configurations of particles were made by Kranendonk and Frenkel.[50] This simulation method has been further generalized to restricted geometry and to the implementation of the grand canonical ensemble Monte Carlo (MC) simulation.[51–54] In our recent works,[55–57] we have extended the simulation studies of pure adhesive fluid to the symmetric[55,56] and asymmetric[57] binary mixtures. The structure of the bulk symmetric binary mixture and its adsorption in planar pores has been investigated in the works of Refs. 55 and 56, respectively, while the very recent article of Ref. 57 reports on the structural study of the bulk two-component system of SHS fluids with the size asymmetry of the particles of both components. In the present work, MC simulation and PY theory are used to investigate the structural properties of such two-component SHS system, mimicking an asymmetric binary colloidal mixture, near a planar wall.

2. Model and Methods

2. 1. Model

The model comprises a mixture of sticky hard-sphere fluids confined between two plane, parallel, smooth, hard plates of infinite extent. The phase confined in the pore is in equilibrium with the bulk phase characterized by the bulk number densities ρ_i and the chemical potentials μ_i. The walls are parallel to the plane (0, *y, z*) and located at $x = 0$ and $x = L$. The sphere diameter of the species i is σ_i, so only the width $L - \sigma_i$ is available to their centers. When modeling wide enough pores, where there exist domains of the fluid sufficiently distant from both walls to retain practically unperturbed density and other properties of the bulk phase, it can be accepted that the structure of the fluid at either plate does not appear to be affected by the presence of the opposite wall. These results should therefore be almost identical to the density profiles next to isolated walls or walls at infinite separations. This way, the structure of the fluid near a single hard flat interface is considered.

The molecules interact among themselves through the special form of square-well potential $\phi_{ij}(r)$ with the well depth ε_{ij} and width $\sigma_{ij} - \sigma'_{ij}$ where $\sigma_{ij} = (\sigma_i + \sigma_j)/2$, in the limit $\sigma'_{ij} \to \sigma_{ij}$. This corresponds to an infinitely deep and short ranged attractive potential well leading to a finite probability of particles i touching particles j, the Boltzmann factor $\exp(-\beta\phi_{ij})$ having the form of Dirac δ function

$$\exp\left[-\beta\phi_{ij}(r)\right] = \frac{\sigma_{ij}}{12\tau_{ij}}\delta\left(r-\sigma_{ij}^{-}\right) + \Theta\left(r-\sigma_{ij}\right) \qquad (1)$$

Above, $\beta = 1/kT$, where k is the Boltzmann constant and T the temperature, $\Theta(x)$ is the Heaviside unit-step function denoting the prohibition of hard core overlaps, and τ_{ij} is the stickiness parameter related to the strength of adhesion and to the temperature of the system. The adhesion strength between the particles of ith and jth species decays with increasing τ_{ij}, $\tau_{ij} = \infty$ corresponding to the absence of an attractive $i - j$ interaction.

The external wall-fluid hard-core potential ϕ_{wi} is given by

$$\phi_{wi}(x) = \begin{cases} 0, & \frac{\sigma_i}{2} < x < L - \frac{\sigma_i}{2}, \\ \infty, & \text{elsewhere} \end{cases} \qquad (2)$$

where x is the coordinate perpendicular to the walls.

2. 2. Percus-Yevick Approximation for the Multicomponent System of Adhesive Fluids

A detailed theoretical analysis on the structure of confined sticky hard-sphere (SHS) mixture based on the Percus-Yevick (PY)/Ornstein-Zernike (OZ) theory was reported in our previous article.[58] In the following we give a summary of some crucial points accompanying the derivation of the final expression for the calculation of inhomogeneous structure of the SHS mixture in planar pores.

Due to the planar symmetry of the wall-fluid interaction potential, Eq. 2, the average fluid number density in the gap depends only on the perpendicular coordinate x.

The local density $\rho_{wi}(x)$ of ith component is related to the wall-fluid total correlation function $h_{wi}(x)$ by

$$\rho_{wi}(x) = \rho_i \left[1 + h_{wi}(x)\right].$$

We determined $h_{wi}(x)$ by solving the OZ equation for the wall-fluid distribution[59]

$$h_{wi}(x) = c_{wi}(x) + \sum_j \rho_j \int d\mathbf{x}'\, h_{wj}\left(\left|\mathbf{x} - \mathbf{x}'\right|\right) c_{ji}(\mathbf{x}') \quad (3)$$

supplemented by the PY closure relation[60]

$$c_{wi}(x) = \{1 - \exp[\beta\phi_{wi}(x)]\}[h_{wi}(x) + 1] \quad (4)$$

for the wall-fluid correlations. The direct correlation functions c_{ij} we obtained from the PY/OZ integral equation for the fluid-fluid correlations for the SHS mixture in the homogeneous phase, the corresponding analytical expressions derived by using the Baxter's transformation of the OZ equation,[61,45] can be found in our preceding work.[58]

For purely hard-core interactions among the walls and the molecules, the PY relation (4) for the wall-fluid correlations reads:

$$c_{wi}(x) = 0 \text{ at } \frac{\sigma_i}{2} < x < L - \frac{\sigma_i}{2}$$

and

$$h_{wi}(x) = -1 \text{ if } x < \frac{\sigma_i}{2} \text{ or } x > L - \frac{\sigma_i}{2}. \quad (5)$$

For each set of the parameters ρ_i, L and τ_{ij}, the numerical solution of the system of Eqs. 3 for a set of equidistant grid points x within the intervals $½\sigma_i < x < L - ½\sigma_i$ was obtained by the iteration procedure. For each grid point x, the real space convolution integrals over the spheres of radius σ_{ij} with their centers located at x have to be evaluated. The integrands are the products of two differently symmetric functions, $c(r)$ and $h(x)$. In view of the delta function term included in the expressions for the direct correlation function[58] both volume and surface integrations have to be carried out. After a suitable substitution, the system of PY/OZ Eqs. 3 may be rewritten in the form

$$h_{wi}(x) = \sum_j \rho_j \int_{-\sigma_{ij}}^{\sigma_{ij}} h_{wj}(u + x) S_{ji}(u)\, du$$

$$= \sum_j \rho_j \int_{-\sigma_{ij}}^{\sigma_{ij}} h_{wj}(u + x)\, du \cdot 2\pi \int_0^{(\sigma_{ij}^2 - u^2)^{1/2}} c_{ji}\left(\sqrt{R^2 + u^2}\right) R\, dR, \quad \frac{\sigma_i}{2} < x < L - \frac{\sigma_i}{2} \quad (6)$$

where the functions $S_{ij}(u)$:

$$S_{ji}(u) = 2\pi \int_0^{(\sigma_{ij}^2 - u^2)^{1/2}} c_{ji}\left(\sqrt{R^2 + u^2}\right) R\, dR \quad (7)$$

denote the analytic integrals over the areas of the circles of radius $(\sigma_{ij}^2 - u^2)^{½}$. As the functions c_{ij} are related only to the bulk system, the values of the integrals $S_{ij}(u)$ can be tabulated prior to the iteration procedure, the resulting final analytic expressions can be found in our previous work.[58]

2. 3. Monte Carlo Simulation

The adhesive potential described by Eq. 1 implies finite probabilities of contact configurations between molecular pairs. This property is related to the infinite depth of contact intermolecular potential, a feature that cannot be captured by the conventional Monte Carlo (MC) method with particles moving at random in a three-dimensional space. This problem has been overcome by monitoring the particle motion in a transformed configurational space where finite volumes were being assigned to the energetically favored binding configurations.[50] Each move involving zero to triple bonded states corresponds to a move within the three-dimensional subvolumes of the rescaled configurational phase space in which the volume elements are expanded in proportion to the Boltzmann factors of a specified configuration. A detailed description of the Kranendonk-Frenkel method for the simulation of a single SHS fluid is to be found in their original paper[50] as well as in the recent works of Miller and Frenkel.[52–54] In our recent works[55–57] we reported on the first simulation studies of the SHS mixtures. The main features of the canonical[55,57] and grand canonical[56] simulation of the asymmetric two-component SHS system are briefly described in the Appendix.

3. Numerical Results and Discussion

The values of the stickiness parameters τ_{ij} can be thought of as being a measure of either the strength of adhesion or the temperature of the system. In order to avoid this uncertainty and to make contact with reality, the adhesive potential is usually related to a more realistic potential, say ϕ_{ij}, via the second virial coefficients. In this way, a system with the potential ϕ_{ij} is actually modeled by the analytically tractable SHS system.[48,58] Matching the second virial coefficients of both systems, the dependence of τ_{ij} upon temperature is given by

$$\frac{\sigma_{ij}^3}{12\tau_{ij}} = \frac{\sigma_{ij}^3}{3} + \int_0^\infty r^2 \left[\exp\left(-\beta\phi_{ij}^{\text{real}}\right) - 1\right] dr\,. \quad (8)$$

Similarly as in our previous works,[48,58] we use the truncated Lennard-Jones (LJ) potential ϕ_{ij}^{LJ} for ϕ_{ij}^{real} defined by the equation

$$\phi_{ij}^{\text{LJ}}(r) = 4\varepsilon_{ij}\left[\left(\frac{\sigma_{ij}}{r}\right)^{12} - \left(\frac{\sigma_{ij}}{r}\right)^{6}\right], \quad r < A$$
$$= 0, \qquad\qquad\qquad\qquad r > A, \tag{9}$$

together with the Berthelot rule for the cross-interaction parameter of the depth of the potential well

$$\varepsilon_{ij} = \left(\varepsilon_{ii} \cdot \varepsilon_{jj}\right)^{1/2}. \tag{10}$$

In the present work we examine the SHS mixture with the following values of the stickiness parameters τ_{ij} : $\tau_{11} = 0.204$, $\tau_{22} = 0.448$, and $\tau_{12} = 0.304$. These values were obtained by matching the second virial coefficients for SHS potential and truncated LJ potential (the range A is given the value $10\sigma_{ij}$) for the temperature T = 300K and LJ energy parameters $\varepsilon_{ij}^{*} = \varepsilon_{ij}/k$, ε_{11}^{*} = 125 K and $\varepsilon_{22}^{*} = 60$ K. The size of the molecules of component 1 is σ_1 and that of the molecules of component 2 is $\sigma_2 \geq \sigma_1$. The composition of the mixture is expressed in terms of the mole fraction $x_1 = \rho_1/\rho$, where ρ_1 is the number density of component 1 and $\rho = \rho_1 + \rho_2$ the corresponding value for the total number density. The reduced density $\rho^{*} = \rho\sigma_1^3$ is

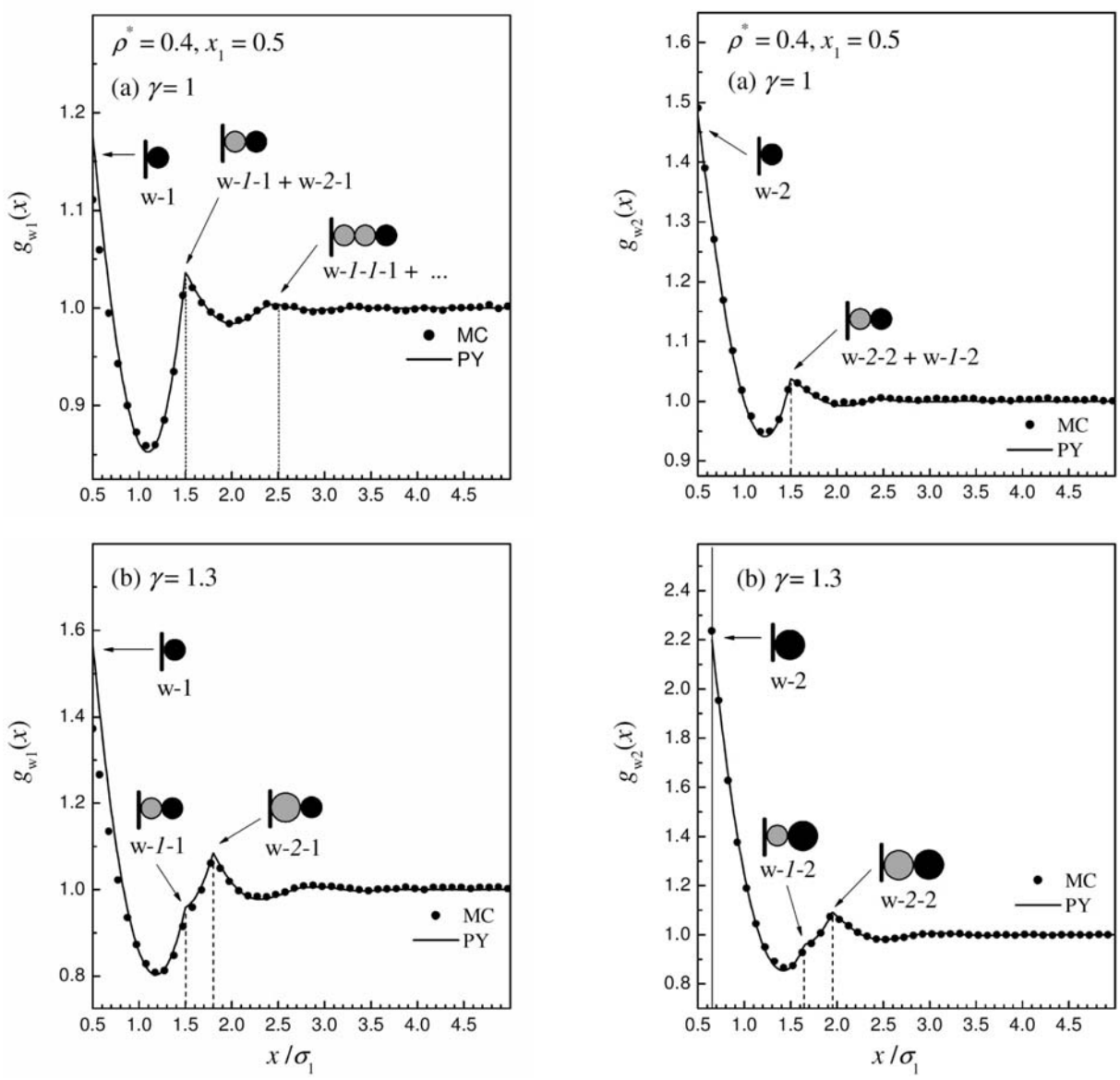

Figure 1. The PY (lines) and MC (symbols) one-particle distribution functions $g_{w1}(x)$ and $g_{w2}(x)$ of the binary SHS mixtures near a single hard wall at the values of the stickiness parameters $\tau_{11} = 0.204$, $\tau_{22} = 0.448$, and $\tau_{12} = 0.304$, at different values of the diameter ratio $\gamma = \sigma_2/\sigma_1$. The systems are in equilibrium with bulk phases of total reduced density $\rho^{*} = 0.4$ and composition $x_1 = 0.5$. Insets: The sketches depict the structures indicating the distances from the wall (w) to the darker particles, which correspond to the particular marked positions on the curves. The smaller and bigger spheres represent the smaller molecules of component 1 and the bigger molecules of component 2, respectively.

used in the following discussion and σ_1 is chosen for the length unit. The parameters B_1 and B_2 entering the simulation of the bulk system were adjusted to the values, which resulted in the equimolar composition $x_1 = 0.5$ and total bulk densities $\rho = 0.2$ and 0.4, respectively.

In Figures 1 and 2 we present the MC and PY one-particle wall-fluid distribution functions of particular components $g_{wi}(x) = \rho_{wi}(x)/\rho_i$ of the SHS mixtures near a single hard wall. Individual figures are subdivided into parts (a)-(b) and (a)-(c), respectively, which successively illustrate the effect of increase in the diameter ratio $\gamma = \sigma_2/\sigma_1$. The fluid mixture at the planar interface is in equilibrium with the bulk phase of equimolar composition $x_1 = 0.5$ and the bulk total density $\rho^* = 0.4$ (Fig. 1) and $\rho^* = 0.2$ (Fig. 2). In order to distinctly see the detailed structure of the particular components, different scales are used for ordinate axes in individual parts of the graphs showing g_{w1} (first column) and g_{w2} (second column), respectively. Numerous articles in the literature reported the results for the structure and phase behavior of fluid mixtures at interfaces and in confined systems. A general feature found for the structure of the fluids was their spatial inhomogeneity as a consequence of the packing effects of fluid molecules in the domain close to the wall(s). The actual shape of the density profiles, which characterizes this inhomogeneity, depends on the specific nature of the fluid-fluid and the wall-fluid interactions, and on the degree and geometry of confinement. When an inhomogeneous structure of the fluid stem from the presence of a single wall or wide enough gap, flat density profiles are restored at sufficient distances from the wall(s), irrespective of the specific nature of the intermolecular potential of interactions. Upon approaching the wall these interactions begin to compete with steric effects. This competition, of course, is now strongly dependent on the particular intermolecular potential and, in addition, on the temperature of the system. Whereas the strongly attractive molecules prefer the regions offering better chance for mutual attraction, i.e., away from the hard obstacles or confined system, just the opposite behavior is observed for the molecules interacting through weaker attractive or even purely repulsive interaction potential. Clearly, the latter molecules try to avoid each other and as such they prefer the regions adjacent to the walls of the confinement. Such molecules are therefore accumulated next to the walls to a greater extent than those incorporating stronger attractive interactions. This gives rise to more pronounced packing effects leading to more distinct layering structure and higher wall-fluid contact density of the fluid with weakly attractive or purely repulsive particles. The density profiles of individual components of the mixture were found to be oscillatory with periods equal to the particular sizes of the particles. Besides these general characteristics regarding the structure of fluid(s) subjected to different external fields caused by the presence of various spatial constraints, additional features are observed in the inhomogeneous structure of adhesive fluid as a consequence of the impulse character of SHS intermolecular potential. As all the stickiness parameters τ_{11}, τ_{22}, and τ_{12} take finite values, the tendency of the molecules of both components towards association competes with steric effects. The sticky molecules have a better chance for adhesive intermolecular interaction at sufficient distance from the wall. This tendency is clearly more pronounced in the case of component 1 due to the stronger 1–1 adhesion corresponding to a lower value of the stickiness parameter τ, i.e. $\tau_{11} < \tau_{22}$. The molecules of weakly adhesive component 2 are therefore accumulated next to the walls to a greater extent, thus giving rise to the higher contact densities and higher amplitude of oscillations in the wall-component 2 density profiles. Consequently, the molecules of component 1 are driven away from the wall. Besides the steric effects, the overall pictures of the profiles of both components are, of course, determined by the combination of the strength of attraction among all the possible species pairs. The effect of partial exclusion of component 1 from the region adjacent to the walls are thus opposed by the 2–1 adhesion (finite τ_{12}) among the molecules 1 and those from the denser and highly layered component 2 in the vicinity of the wall. The distribution of molecules of component 2, on the other hand, is similarly affected by the formally identical 1–2 adhesive interaction. In the case of symmetry in size of the molecules of both components [(a) parts of the figures], the isotherm slopes (the first derivative of g_{wi} on x) of both components show discontinuities at distances from the wall/fluid contact plane, which are multiples of the molecular size $\sigma_1 = \sigma_2 = 1$, similarly as observed in the case of a pure adhesive fluid.[51] This is a result of the delta-function peak in the radial distribution function $g_{ij}(r)$ at $r = \sigma_1 = \sigma_2 = \sigma_{12}$, reflecting the finite probability of 1–1, 2–2, and 1–2 contact configurations. In the asymmetrical case, $\gamma > 1$ [(b) and (c) parts of the figures], these discontinuities appear at the distances $n \cdot \sigma_1 + m \cdot \sigma_2$ ($n = 0,1,2,...$; $m = 0,1,2, ...$) from the wall/component 1 and wall/component 2 contact planes as a consequence of the formation of successive molecular layers with two different molecular sizes σ_1 and σ_2, the exception being the combination $n = 0$, $m = 0$. Let us take, for instance, the correlation function $g_{w1}(x)$. The discontinuities at $x = \sigma_1/2 + n \cdot \sigma_1$ result from the 1–1 adhesion and refers to the arrangement of parallel molecular layers where the first monolayer, being located adjacent to the wall, is that of component 1 and the successive molecular layers of the same component. The discontinuities at $x = \sigma_1/2 + m \cdot \sigma_2$ stem from the arrangement of m successive molecular layers of component 2 from the wall (the finite probability for the 2–2 contact configuration is the consequence of 2–2 adhesion), the $(m + 1)$-th being that of component 1. One can imagine, of course, any "mixed" arrangement of molecular layers of the two components, thus giving rise the appearance of discontinuities at any combination of n and m. The behavior of $g_{w2}(x)$ may be explained by utilizing the same arguments.

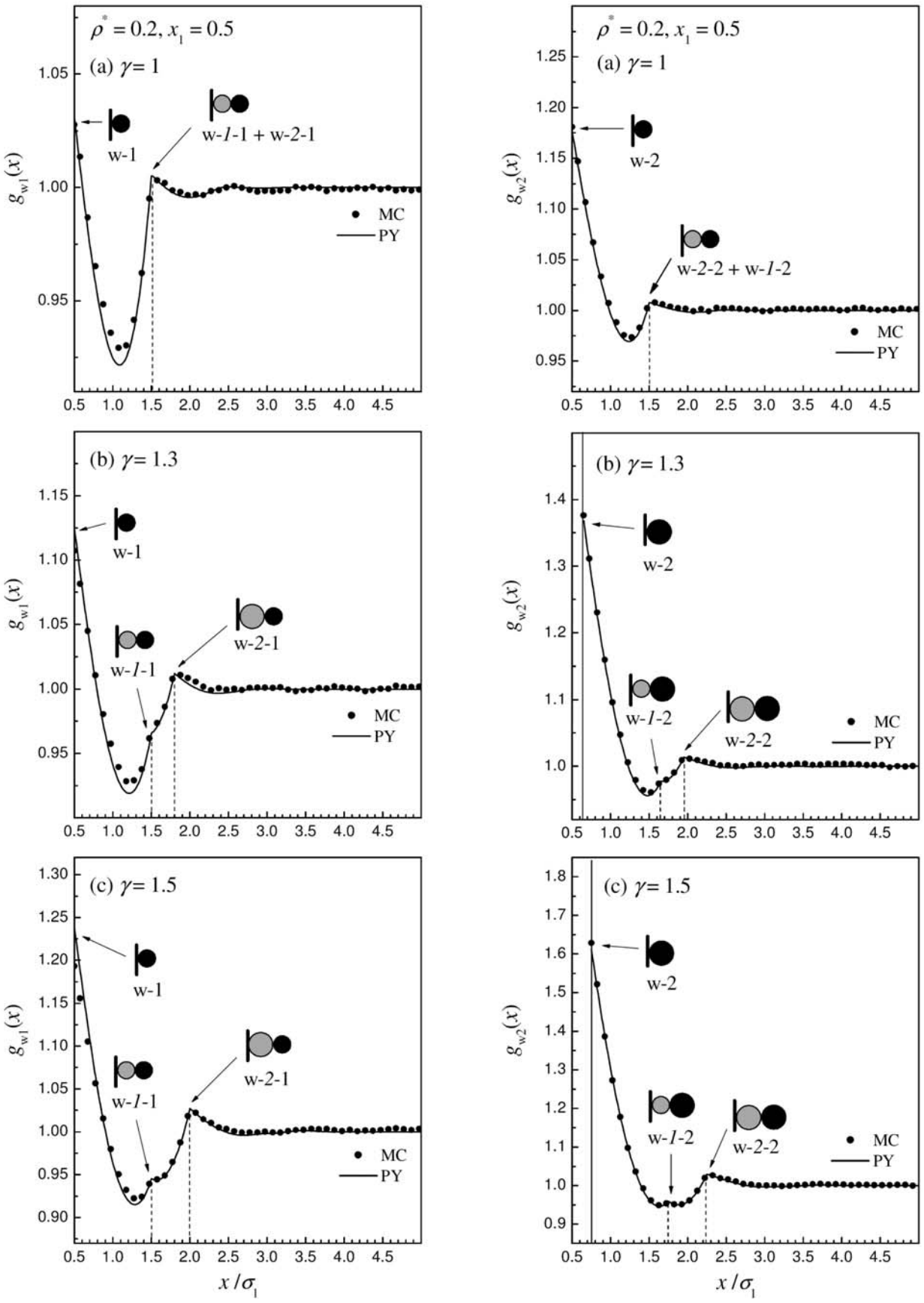

Figure 2. Same as Fig. 1 but for the bulk total reduced density $\rho^* = 0.2$

A comparison of the PY theoretical predictions and the simulation data for the local structures of the SHS mixture at planar interface seen in Figures 1 and 2 indicates fair to very good agreement between the results of both methods. In all cases, the singlet PY theory satisfactorily predicts the structure of the SHS mixture, the exception being the regions in close vicinity to the walls, where somewhat larger discrepancies between the PY and MC results are observed. These discrepancies are more pronounced for the component comprised of strongly adhesive particles. However, we have to stress here that in the present work we consider the SHS mixture at rather mild conditions referring to both the role of the interparticle attraction (adhesion) and exclusion volume effects. At stronger attractive interactions among the molecules and/or for the solution richer in the component containing bigger molecules one can expect that the performance of the theory would considerably worsen, similarly as found for the bulk SHS mixtures studied in our recent paper.[57]

4. Conclusions

In this paper we report grand canonical Monte Carlo simulation and Percus-Yevick studies of the structure of asymmetric two-component sticky hard-sphere (SHS) system, mimicking asymmetric binary colloidal mixture, near a single hard wall. Due to the delta-function in the 1–1, 2–2, and 1–2 interparticle interaction potential the wall-component 1 and wall-component 2 distribution functions exhibit peculiar shapes characterized by successive discontinuities, which appear at the distances equal to the separations of mutually adhered particles of both components. In all cases we found fair to very good agreement between the results of the pure theory and the simulation data.

In future theoretical work, we plan to study the potential of mean force and the solvation force between the sticky colloidal solutes immersed in molecular SHS solvent. As usual, colloid dispersion will be modeled as a multi-component system formed by large (macro)particles mimicking colloidal solute and smaller molecules denoting the solvent component. This way, lyophilic colloidal interactions evidenced experimentally in nonionic colloidal dispersions[62] will be examined.

5. Acknowledgement

The authors thank the support of the Slovenian Research Agency through the Physical Chemistry Research Program 0103-0201.

Appendix: Monte Carlo Simulation of Asymmetric Sticky Hard Sphere Mixtures

In the following paragraphs we briefly sum up the main features of the canonical[55,57] and grand canonical[56] simulation of the asymmetric two-component sticky hard sphere (SHS) system.

A. 1. Canonical Simulation

Motions of particles take place in a transformed configurational space where finite volumes are being assigned to the energetically favored binding configurations.[50] Each move involving zero to triple bonded states corresponds to a move within the three-dimensional subvolumes of the rescaled configurational phase space in which the volume elements are expanded in proportion to the Boltzmann factors of a specified configuration. In the rescaled phase space, the so-called effective volumes of each particular degree of binding cover all the realizations of given type of bond *b* inside the so-called test sphere[50] whose radius is adjusted according to the total density of the fluid mixture. Calculation of the effective volumes in the case of binary SHS mixture claims the consideration of different adhesion strengths τ_{ij} and interparticle contact distances σ_{ij} (*i* and *j* being 1 or 2) corresponding to different contributions of the particles of individual species to the total effective volume for each particular degree of binding. Accordingly, the configurations belonging to the same coordination state, i.e., the same number of contacts, have now different statistical weights. The essential successive steps of the MC algorithm may be outlined as follows:

(1) Choose a particle at random. This 'test particle' may be one of component 1 or one of component 2 with the hard-core diameters σ_1 and σ_2, respectively. We denote it by the index *t*.

(2) Make catalogue of the individual particles, pairs of particles, and particle triplets that allow the formation of single, double, and triple bonds with the test particle inside the test sphere. For all the particles from this list it is necessary to know which of the either components they belong to. On the basis of this list, one calculates the effective volumes for each individual degree of binding taking into account different weights depending on the different adhesive strength acting between like particles of either components or unlike particles, and, in addition, on the different sizes of the particles of individual components. At this calculation, only the parts of the effective volumes located inside the test sphere of volume *V* have to be taken into account. In turn, the effective volume for the formation of single bond (one-contact configuration) is determined by the integral over the available surfaces of other particles,[50,54,57]

$$V_{\mathrm{eff}}^{(1)} = \sum_{\alpha=1}^{2} \frac{\sigma_{t\alpha}}{12\tau_{t\alpha}} \int_{V} \delta(r_{t\alpha} - \sigma_{t\alpha})\, d\mathbf{r}_t \qquad \text{(A1)}$$

where the summation takes into account both components of the binary mixture, which gives rise to two different va-

lues of the pre-integration factor $\sigma_{t\alpha}/12\tau_{t\alpha}$ stemming from different adhesion between like or unlike particles and from different sizes of the particles, i.e., the one corresponding to the adhesion between unlike particles, $\sigma_{12}/12\tau_{12} = \sigma_{21}/12\tau_{21}$, and the other referring to the adhesion between like particles, $\sigma_{11}/12\tau_{11}$ or $\sigma_{22}/12\tau_{22}$ (depending on the test particle, i.e. which component it belongs to). Ignoring for the moment the finite size of the test sphere, the contribution of the particle α to the total effective volume $V_{\text{eff}}^{(1)}$ is[50,54,57]

$$v_{\text{eff},\alpha}^{(1)} = \frac{\sigma_{t\alpha}}{12\tau_{t\alpha}} \times 4\pi\sigma_{t\alpha}^2 \tag{A2}$$

Further, the double bond can be formed when the test particle slips around the circle when simultaneously touching two other particles, α and β. This is possible if the distance between the particles of this particular pair is less than the sum of $t - \alpha$ and $t - \beta$ contact distances, $\sigma_{t\alpha} + \sigma_{t\beta}$. The calculation of the effective volume for the formation of double bond therefore include the integration around the circles obtained in this way for all pairs of other particles from the list, the corresponding expression reads[50,54,57]

$$V_{\text{eff}}^{(2)} = \sum_{\alpha=1}^{2}\sum_{\beta=\alpha}^{2} \frac{\sigma_{t\alpha}}{12\tau_{t\alpha}} \frac{\sigma_{t\beta}}{12\tau_{t\beta}} \int_V \delta(r_{t\alpha} - \sigma_{t\alpha}) \, \delta(r_{t\beta} - \sigma_{t\beta}) \, d\mathbf{r}_t \,, \tag{A3}$$

where the double summation considers all pairs (including the particles of either component) allowing the formation of double bond inside the test sphere. The pre-integration factor now takes three different values referring to the formation of the double bond of test particle with (i) two like particles of the same component, (ii) two like particles of the other component, and (iii) two unlike particles. Therefore, the pair of particles α and β contributes to the total effective volume $V_{\text{eff}}^{(2)}$.[50,54,57]

$$v_{\text{eff},\alpha\beta}^{(2)} = \frac{\sigma_{t\alpha}}{12\tau_{t\alpha}} \frac{\sigma_{t\beta}}{12\tau_{t\beta}} \times 2\pi r_{\alpha\beta} \tag{A4}$$

$r_{\alpha\beta}$ being the radius of the circle formed by points lying on a distance $\sigma_{t\alpha}$ and $\sigma_{t\beta}$ from the particles α and β, respectively. Again only the parts of the circle(s) falling inside the test sphere have to be taken into account. Finally, the effective volume for the possible triple bonds of the test particle with any triplet of particles equals to[50,54,57]

$$V_{\text{eff}}^{(3)} = \sum_{\alpha=1}^{2}\sum_{\beta=\alpha}^{2}\sum_{\gamma=\beta}^{2} \frac{\sigma_{t\alpha}}{12\tau_{t\alpha}} \frac{\sigma_{t\beta}}{12\tau_{t\beta}} \frac{\sigma_{t\gamma}}{12\tau_{t\gamma}} \int_V \delta(r_{t\alpha} - \sigma_{t\alpha}) \, \delta(r_{t\beta} - \sigma_{t\beta}) \, \delta(r_{t\gamma} - \sigma_{t\gamma}) \, d\mathbf{r}_t \,, \tag{A5}$$

with four different values of the pre-integration factor resulting from the above triple summation. These values follow from different combinations of the values of the indices α, β, γ, each taking the value 1 (component 1) or 2 (component 2), i.e., (i) 1,1,1; (ii) 1,1,2 = 1,2,1 = 2,1,1; (iii) 1,2,2 = 2,1,2 = 2,2,1; and (iv) 2,2,2. Contribution of the particular triplet α, β, γ to the total $V_{\text{eff}}^{(3)}$ is given by[50,54,57]

$$v_{\text{eff},\alpha\beta\gamma}^{(3)} = \frac{\sigma_{t\alpha}}{12\tau_{t\alpha}} \frac{\sigma_{t\beta}}{12\tau_{t\beta}} \frac{\sigma_{t\gamma}}{12\tau_{t\gamma}} \times \frac{2}{\left|\mathbf{r}_{t\alpha} \cdot \left(\mathbf{r}_{t\beta} \times \mathbf{r}_{t\gamma}\right)\right|} \tag{A6}$$

$\mathbf{r}_{t\alpha}$, $\mathbf{r}_{t\beta}$, and $\mathbf{r}_{t\gamma}$ are the unit vectors along the directions of the vectors joining the center of the test particle to the centers of the other three particles, α, β, and γ. With the factor 2 in the above Eq. A6 the two equivalent contributions with the test particle touching the particles of the triplet from both sides are taken into account. The effective volume for a free move of the test particles without forming any bond with other particles is just the volume of the test sphere, $V_{\text{eff}}^{(0)} = V$.

(3) Calculate the transition probabilities for each type of bond b (b ranging from 0 to 3) and select a particular configuration with the weight equal to its transition probability

$$P(b) = \frac{V_{\text{eff}}^{(b)}}{\sum_{b=0}^{3} V_{\text{eff}}^{(b)}}, \tag{A7}$$

(4) Randomly choose a position within the region of space corresponding to the selected type of bond. Here, consider different weights caused by different strength of adhesion between the test particle and other particles and by different sizes of the particles for this (selected) degree of binding.

(5) Accept the new configuration unless a hard-core overlap has been detected.

A. 2. Grand Canonical Simulation

In the open ensemble, the chemical potentials of the individual components μ_i, the volume V, and the temperature T of the system are fixed, while the numbers of particles N_i are allowed to fluctuate. This set of independent parameters that define the thermodynamic state of the system makes possible the study of equilibrium between the SHS mixture in the homogeneous phase and the same mixture being subjected to some external potential. The latter, in our case, was imposed by the presence of two parallel, perfectly smooth hard walls at a specified separation L mimicking a planar slit. The actual distances accessible for the individual components of the confined SHS mixture were therefore $L - \sigma_i$. Denoting the perpendicular direction by x, the fluid mixture between the walls extended to infinity along the directions y and z, parallel to the

walls. In practical simulations, the system was modeled as an infinite array of identical simulation cells of the volume $L \times a^2$, repeating themselves in the two lateral directions, along which the minimum image convention was applied. No periodicity needed to be assumed in the direction x normal to the plates. In addition, when modeling wide enough pores, where there exist domains of the fluid sufficiently distant from both walls to retain practically unperturbed density and other properties of the bulk phase, it could be accepted that the structure of the fluid at either plate did not appear to be affected by the presence of the opposite wall. These results should therefore be almost identical to the density profiles next to isolated walls or walls at infinite separations. This way, the structure of the SHS mixture near a single hard, flat interface was considered. In most cases, the value for the width of the gap L about ten molecular diameters was sufficient to avoid the interference between the symmetrical density profiles at individual walls of the pore.

During the simulation, the phase space was sampled through alternating canonical (CMC) and grand canonical (GCMC) steps, i.e. by the movement of randomly chosen particle, and by the addition to or removal of particles from the system. Additions and removals were attempted randomly with a probability P, so the probability for a move of a randomly chosen particle was $1 - 2P$. The value $P \approx 0.15$ was used in most of our runs. The general features of the GCMC method are described elsewhere.[63] Further, details peculiar to the GCMC simulation of the one-component SHS fluid were discussed in our previous work[51] and in the recent works of Miller and Frenkel.[53,54] Here we only resume some essential characteristics concerning the simplification of the GCMC algorithm and give some points regarding the extension to the GCMC simulation of SHS mixture. In the case of SHS system, each addition or removal of a particle may be accompanied by the formation or by the breaking of the bond(s). For this reason, the standard GCMC relations[63] for the acceptance probability of an attempted addition and deletion, respectively, should be suitably modified. Similarly as has been noted in the context of CMC simulation, the effective volumes $V_{\mathrm{eff}}^{(b)}$ for the specified binding states of the particle should be calculated. Unlike the CMC simulation, where the calculation of $V_{\mathrm{eff}}^{(b)}$ is restricted to the interior of a suitably chosen test sphere, which is much smaller than the entire MC cell, the effective volumes should, in principle, be determined for the entire MC cell at each GCMC step. This would, of course, consume a prodigious amount of computer time, especially at high densities where the number of available binding configurations may be extremely large. For this reason, we prefer to add and remove only non-associated particles and let the number of bonds adjust through internal equilibration during the CMC steps, similarly as proceeded in the case of the GCMC simulation of the one-component SHS fluid.[51,53,54] This simplification leads to the expression for the acceptance probability quite similar to that of the standard method,[63] the only difference being in considering only a fraction of the entire number of particles, i.e. the non-bounded particles, denoted by the indexes 0. Chemical potentials of individual species of the whole system, μ_i, and of non-bounded particles, $\mu_{i,0}$, are given by

$$\beta\mu_i = \ln \Lambda_i^3 + \ln\langle \rho_i \rangle + \beta\mu_i^{ex}$$
and (A8)
$$\beta\mu_{i,0} = \ln \Lambda_i^3 + \ln\langle \rho_{i,0} \rangle + \beta\mu_{i,0}^{ex}$$

where the terms $\ln \Lambda_i^3$ are related to constant kinetic contributions, Λ_i being the de Broglie thermal wavelengths. $\langle \rho_i \rangle$ and $\langle \rho_{i,0} \rangle$ are the average densities whereas μ_i^{ex} and $\mu_{i,0}^{ex}$ denote the excess chemical potentials of i-th component. Considering the chemical potentials of non-bounded particles of individual species to be equal to those of the whole system, the following expression for the new parameters B_i, which are kept constant during the simulation, are obtained:

$$B_i = \beta\mu_i - \ln \Lambda_i^3 = \beta\mu_i^{ex} + \ln\langle \rho_i \rangle = \beta\mu_{i,0}^{ex} + \ln\langle \rho_{i,0} \rangle \quad \text{(A9)}$$

The acceptance probabilities of attempted additions $f_{i,0}^{(mn)}$ or of deletions $f_{i,0}^{(nm)}$ of the non-bounded particles of individual species, where $N_{i,0}^{(n)} = N_{i,0}^{(m)} + 1$, read[51,56]

$$f_{i,0}^{(mn)} = r_i\,, \quad f_{i,0}^{(nm)} = 1 \quad \text{if } r_i \le 1$$
$$f_{i,0}^{(mn)} = 1\,, \quad f_{i,0}^{(nm)} = r_i^{-1} \quad \text{if } r_i > 1 \quad \text{(A10)}$$

with

$$r_i = \frac{V}{N_{i,0}^{(n)}} \exp\left[B_i - \beta \Delta u_i^{(mn)} \right] \quad \text{(A11)}$$

where the energy changes due to additions or deletions of non-associated particles of individual species $\Delta u_i^{(mn)}$ equal zero. This procedure is therefore identical to that used for ordinary hard sphere fluid. From the values of B_i and the average densities $\langle \rho_i \rangle$, which result from the simulation of the bulk system, the excess chemical potentials μ_i^{ex} of the individual components of the SHS mixture and the corresponding values for the non-bounded particles $\mu_{i,0}^{ex}$ can be obtained. As fixing B_i is equivalent to fixing μ_i the same values of B_i are then used in the GCMC simulation of the SHS mixture under the influence of external field.

6. References

1. S. Bhattacharya, J. Blawzdziewicz, *J. Chem. Phys*. **2008**, *128*, 214704.
2. Y. Vandecan, J. O. Indekeu, *J. Chem. Phys*. **2008**, *128*, 104902.
3. W. Li, T. Yang, H. R. Ma, *J. Chem. Phys*. **2008**, *128*, 044910.
4. S. L. Eichmann, S. G. Anekal, M. A. Bevan, *Langmuir* **2008**, *24*, 714–721.

5. R. E. Beckham, M. A. Bevan, *J. Chem. Phys*. **2007**, *127*, 164708.
6. H. Reich, M. Dijkstra, R. van Roij, M. Schmidt, *J.Phys. Chem. B* **2007**, *111*, 7825–7835.
7. S. G. Anekal, M. A. Bevan, *J. Chem. Phys*. **2006**, *125*, 034906.
8. A. Fortini, M. Schmidt, M. Dijkstra, *Phys. Rev. E* **2006**, *73*, 051502.
9. A. Fortini, M. Dijkstra, M. Schmidt, P.P. Wessels, *Phys. Rev. E* **2005**, *71*, 051403.
10. J. M. Brader, M. Dijkstra, R. Evans, *Phys. Rev. E* **2001**, *73*, 041405.
11. A. Trokhymchuk, D. Henderson, A. Nikolov, D. T. Wasan, *Phys. Rev. E* **2001**, *64*, 012401.
12. J. Siodmiak, A. Gadomski, E. Pechkova, C. Nicolini, *Intern. J. Mod. Phys. C* **2006**, *17*, 1359–1365.
13. J. J. Cerda, T. Sintes, C. Holm, C. M. Sorensen, A. Chakrabarti, *Phys. Rev. E* **2008**, *78*, 031403.
14. G. Foffi, L. Angelani, *J. Phys.: Condens. Mat.* **2008**, *20*, 075108.
15. P. Charbonneau, D. R. Reichman, *Phys. Rev. E* **2007**, *75*, 050401.
16. M. Sztucki, T. Narayanan, G. Belina, A. Moussaid, F. Pignon, H. Hoekstra, *Phys. Rev. E* **2006**, *74*, 051504.
17. A. Coniglio, L. de Arcangelis, A. de Candia, E. Del Grado, A. Fierro, N. Sator, *J. Phys.: Condens. Mat.* **2006**, *18*, S2383–S2390.
18. R. J. Baxter, *J. Chem. Phys*. **1968**, *49*, 2770–2774.
19. D. Gazzillo, A. Giacometti, *J. Chem. Phys*. **2004**, *120*, 4742–2754.
20. D. W. Marr, A. P. Gast, *J. Chem. Phys*. **1993**, *99*, 2024–2031.
21. K. Shukla, R. Rajagopalan, *Mol. Phys*. **1994**, *81*, 1093–1107.
22. K. Shukla, R. Rajagopalan, *Int. J. Thermophys*. **1995**, *16*, 327–335.
23. A. Jamnik, D. Bratko, D. Henderson, *J. Chem. Phys*. **1991**, *94*, 8210–8215.
24. M. H. G. M. Penders, A. Vrij, *Physica A* **1991**, *173*, 532–547.
25. A. Jamnik, D. Bratko, *Vestn. Slov. Kem. Drus*. **1991**, *38*, 39–53.
26. A. Jamnik, *Chem. Phys. Lett*. **1998**, *292*, 481–486.
27. A. Jamnik, *J. Chem. Phys*. **1998**, *109*, 11085–11093.
28. J. N. Herrera, L. Blum, *Nuovo Cimento D* **1994**, *16*, 703–709.
29. S. Buzzaccaro, R. Rusconi, R. Piazza, *Phys. Rev. Lett*. **2007**, *99*, 098301.
30. R. Chiarizia, P. G. Rickert, D. Stepinski, P. Thiyagarajan, K. C. Littrell, *Solvent Extr. Ion Exc*. **2006**, *24*, 125–148.
31. R. Chiarizia, M. P. Jensen, P. G. Rickert, Z. Kolarik, M. Borkowski, P. Thiyagarajan, *Langmuir* **2004**, *20*, 10798–10808.
32. S. Nave, C. Mandin, L. Martinet, L. Berthon, F. Testard, C. Madic, T. Zemb, *Phys. Chem. Chem. Phys.* **2004**, *6*, 799–808.
33. R. Chiarizia, K. L. Nash, M. P. Jensen, P. Thiyagarajan, K. C. Littrell, *Langmuir* **2003**, *19*, 9592–9599.
34. K. Li, H. Guo, Z. Q. Liang, P. Thiyagarajan, Q. Wang, *J. Polym. Sci. Pol. Chem*. **2005**, *43*, 6007–6019.
35. C. Gehin, J. Persello, D. Charraut, B. Cabane, *J. Colloid Interf. Sci.* **2004**, *273***,** 658–667.
36. G. Cassin, Y. Duda, M. Holovko, J.P. Badiali, M. P. Pileni, *J. Chem. Phys.* **1997**, *107*, 2683–2693.
37. M. F. Holovko, E. V. Vakarin, Y. Y. Duda, *Chem. Phys. Lett.* **1995**, *233*, 420–423.
38. I. A. Protsykevich, Y. Duda, M. F. Holovko, *Chem. Phys. Lett.* **1996**, *248*, 57–62.
39. E. Vakarin, Y. Duda, M. Holovko, *J. Chem. Phys.* **1997**, *107*, 5569–5581.
40. Y. Duda, S. Sokolowski, P. Bryk, O. Pizio, *J. Phys. Chem. B* **1999**, *103*, 5490–5494.
41. F. Jimenez-Angeles, Y. Duda, G. Odriozola, M. Lozada-Cassou, *J. Phys. Chem. C* **2008**, *112*, 18028–18033.
42. A. Jamnik, D. Bratko, *Chem. Phys. Lett.* **1993**, *203*, 465–471.
43. A. Jamnik, *J. Chem. Phys*. **1995**, *102*, 5811–5817.
44. B. Barboy, *Chem. Phys*. **1975**, *11*, 357–371.
45. B. Barboy, R. Tenne, *Chem. Phys*. **1979**, *38*, 369–387.
46. C. Tutschka, G. Kahl, *J. Chem. Phys*. **1998**, *108*, 9498–9505.
47. E. Dickinson, *J. Chem. Soc. Faraday Trans*. **1995**, *91*, 4413–4417.
48. A. Jamnik, *J. Chem. Phys*. **1996**, *105*, 10511–10520.
49. S. Amokrane, C. Regnaut, *J. Chem. Phys*. **1997**, *106*, 376–387.
50. W. G. T. Kranendonk, D. Frenkel, *Mol. Phys*. **1988**, *64*, 403–424.
51. A. Jamnik, D. Bratko, *Phys. Rev. E* **1994**, *50*, 1151–1161.
52. M. A. Miller, D. Frenkel, *J. Phys.: Condens. Mat*. **2004**, *16*, S4901–S4912.
53. M. A. Miller, D. Frenkel, *Phys. Rev. Lett.* **2003**, *90*, 135702.
54. M. A. Miller, D. Frenkel, *J. Chem. Phys*. **2004**, *121*, 535–545.
55. A. Jamnik, *Chem. Phys. Lett*. **2006**, *423*, 23–29.
56. A. Jamnik, *J. Phys. Chem. B* **2007**, *111*, 3674–3684.
57. A. Jamnik, *J. Chem. Phys*. **2008**, *128*, 234504.
58. A. Jamnik, *J. Chem. Phys*. **2001**, *114*, 8619–8627.
59. D. Henderson: Fundamentals of Inhomogeneous Fluids, Dekker, New York, **1992**.
60. H. L. Friedman: A Course in Statistical Mechanics, Prentice Hall, Engelwood Cliffs, NJ, **1985**.
61. R. J. Baxter, *J. Chem. Phys*. **1970**, *52*, 4559–4562.
62. J. N. Israelachvili: Intermolecular and Surface Forces, Academic Press, London, NJ, **1985**.
63. D. Frenkel, B. Smit: Understanding Molecular Simulation, Academic Press, Boston, MA, **1996**.

Povzetek

V pričujočem delu smo raziskovali vpliv zunanjega polja (toge ravne stene) na strukturo dvo-komponentne asimetrične mešanice modelnih tekočin z adhezivnim medmolekulskim potencialom, ki ponazarja binarni sistem interagirajočih koloidnih delcev v suspenziji. Nehomogeni (omejeni) koloidni sistem je bil v ravnotežju z homogenim (neomejenim) sistemom. Prostorske korelacije stena-komponenta 1 in stena komponenta 2 smo obravnavali z velekanonično simulacijo Monte Carlo in z Ornstein-Zernike-ovo integralsko enačbo v Percus-Yevick-ovem približku. Svojska oblika gostotnih profilov posameznih komponent je posledica zapletenih vzajemno delujočih interakcij stena-molekule ter adhezivnih parskih medmolekulskih interakcij 1–1, 2–2 in 1–2. Zaradi impulznega karakterja adhezivnega potenciala so ti na razdaljah med steno in molekulami, ki so enake različnim vsotam večkratnikov premerov molekul posameznih komponent, nezvezni. Primerjava med rezultati simulacije in napovedmi PY teorije kaže na skoraj kvantitativno ujemanje rezultatov obeh metod. Ker uspešnost teorije pojema z naraščajočo jakostjo privlačnih medmolekulskih interakcij, se v primeru adhezivne mešanice teorija bolje obnese za komponento šibkeje adhezivnih molekul.